



# High polarisation extinction ratio of the TM-pass polariser with silicon carbide/graphene/silicon multilayers

XINYU WANG<sup>1,2</sup>, WEI SU<sup>1</sup> \* and XINGYU LIU<sup>1,2</sup>

<sup>1</sup>Department of Mathematics and Physics, Hohai University, Changzhou Campus, Changzhou 213022, China

<sup>2</sup>College of Mechanical and Electrical Engineering, Hohai University, Changzhou 213022, China

\*Corresponding author. E-mail: opticSu@hotmail.com

MS received 7 March 2019; revised 21 June 2019; accepted 17 July 2019; published online 4 October 2019

**Abstract.** We propose a compact TM-pass polariser, consisting of silicon (Si)/silicon carbide (SiC)/Si layers. Two graphene sheets are sandwiched between the Si and SiC layers as the interlayer to enhance the interaction with light. The loss characteristics have been investigated by using the finite-difference time-domain (FDTD) method. The proposed structure exhibits a low insertion loss (IL) of  $\sim 0.25$  dB and a high polarisation extinction ratio (PER) of  $\sim 57$  dB. To verify the robustness of the proposed polariser, we analyse the fabrication tolerance of the waveguide width and the height of the Si and SiC layers. The polariser shows great fabrication error tolerance. In addition, by employing a  $100\ \mu\text{m}$  long waveguide, a PER of 48.3–59.4 dB is obtained in the visible regime ranging from 400 to 600 nm.

**Keywords.** Polariser; graphene; high extinction ratio.

**PACS Nos** 02.60.Cb; 42.25.Bs; 42.25.Ja

## 1. Introduction

For the past few years, silicon photonics has been widely used in photonics-integrated circuits. Because of the small size, high integration ability and low cost, silicon photonics has attracted worldwide interest [1]. At the same time, silicon photonics is expected to be used in super-high-speed internet access [2]. However, due to the high index contrast of silicon photonic devices, they always cause large structural birefringence leading to polarisation-dependent loss, greatly limiting their practical use [3]. To solve this problem, a polarisation diversity scheme is often employed, such as polarisation splitters [4], rotators [5], and polarisers [6–8] are usually used as building blocks. Among them, the polarisers are commonly used to build polarisation transparent circuits.

It needs to be pointed out that optical polarisers are one of the most important devices in optic communications because more and more optical components have been used on the polarisation states [9]. These are essential components in many applications such as information security, polarimetric imaging [10], nano-, bio-, and chemical-sensors [11], mobile display [12], and machine vision [13]. High-performance

polarisers should have high polarisation extinction ratio (PER), low insertion loss (IL), and small footprint [14]. The transreflector polarisers (TRPs) which reflect or absorb one polarisation can be divided into two main categories: free-standing or laminate polarisers and substrate polarisers [15]. The most common TRPs are free-standing polarisers, which can split the unpolarised input waves into two polarised beams and pass the desired polarisation while reflecting the other [16].

Graphene is well-known as a two-dimensional material made of carbon atoms, which is the basic material in electronics, plasmonics, and photonics, due to its high electron mobility, optical transparency, and high flexibility [17–19]. Graphene is a popular material which has great electronic and mechanic properties [20,21]. The performance of the optical devices based on graphene can be tuned by the Fermi level of the graphene sheet, and the graphene integrated with a silicon waveguide can greatly enhance light interaction [22–24]. For example, in ref. [25], a TE-pass polariser based on a silicon slot waveguide with graphene multilayer at  $1.55\ \mu\text{m}$  is proposed. The TM-mode IL is  $\sim 31.5$  dB and the TE-mode IL is  $\sim 0.2$  dB. In ref. [26], a graphene–silicon-based TM-pass polariser has been investigated. The PER is  $\sim 40$  dB and the IL is  $\sim 3$  dB at the wavelength range

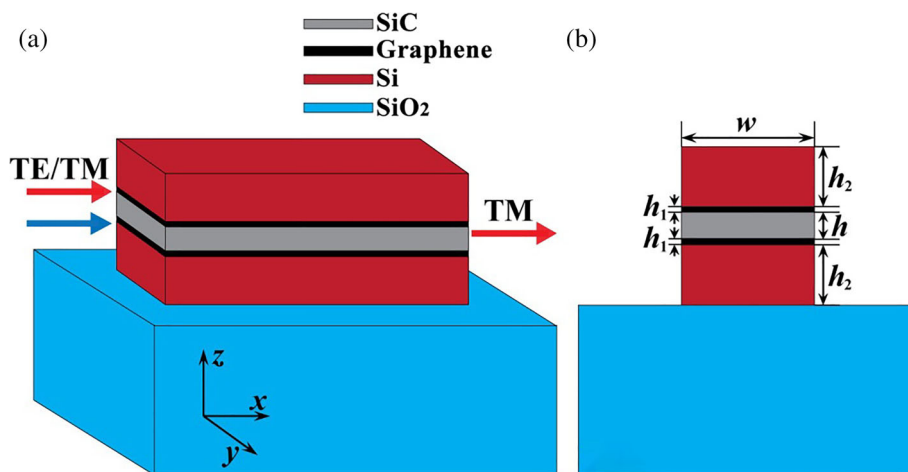


**Figure 1.** (a) 3D schematic of the proposed TM-pass polarizer and (b) sectional view of the polariser.

1450–1650 nm. Most of the reported polarisers based on graphene material are used in infrared and terahertz bands, but a few of them are designed for visible spectrum.

In this paper, we propose a compact TM-pass polariser with the working wavelength in the visible range, which utilises the electro-absorption effect of graphene. The structure consists of Si/SiC/Si layers, with the graphene sheet as the interlayer to enhance the interaction with light. The relationship between loss characteristics and the structure parameters has been investigated by using the three-dimensional (3D) finite-difference time-domain (FDTD) method, which shows great fabrication error tolerance. In addition, the proposed polariser exhibits high PER and low IL in the visible regime ranging from 400 to 600 nm.

## 2. Model and discussions

Figure 1 shows the 3D schematic and sectional view of the proposed TM mode-pass polariser.  $w$  is the width of the total waveguide.  $h$ ,  $h_1$ , and  $h_2$  are the heights of the SiC, graphene, and Si layers, respectively. The two graphene sheets are sandwiched between the Si and SiC layers, to form the Si/graphene/SiC/graphene/Si waveguide structure. The refractive indices of Si and SiC are taken from experimental measurements [27]. The dielectric constant of graphene can be calculated as follows [28]:

$$\varepsilon(\omega) = 1 + \frac{i\sigma(\omega)}{\omega\varepsilon_0\Delta}, \quad (1)$$

where  $\omega$  is the radian frequency,  $\varepsilon_0$  is the vacuum permittivity,  $\Delta$  is the thickness of the graphene layer, and  $\sigma(\omega)$  is the complex surface conductivity. Here the complex

surface conductivity can be calculated from the Kubo formula as follows [29]:

$$\begin{aligned} \sigma(\omega) &= \sigma_{\text{intra}}(\omega) + \sigma_{\text{inter}}(\omega) \\ &= \frac{2e^2k_B T}{\pi\hbar^2} \ln \left[ 2\cosh\left(\frac{\mu_c}{2k_B T}\right) \right] \frac{i}{\omega + i\tau^{-1}} \\ &\quad + \frac{e^2}{4\hbar} \left[ H\left(\frac{\omega}{2}\right) + \frac{4i\omega}{\pi} \int_0^\infty \frac{H(\varepsilon) - H(\omega/2)}{\omega^2 - 4\varepsilon^2} d\varepsilon \right], \quad (2) \end{aligned}$$

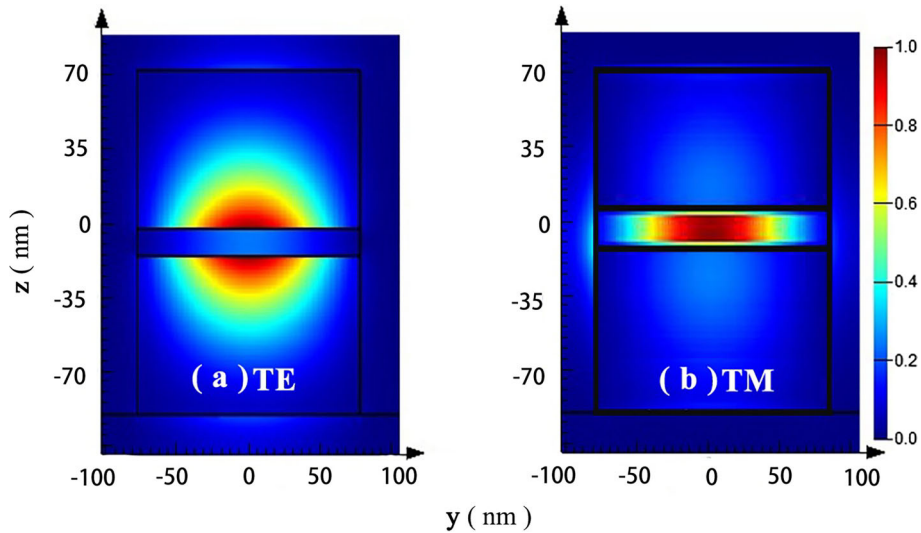
where  $e$  is the charge of an electron,  $k_B$  is the Boltzmann's constant,  $\hbar = h/2\pi$  is the Planck's constant,  $\mu_c$  is the chemical potential,  $T$  is the temperature, and  $\tau$  is the momentum relaxation.

In the following numerical simulations and analysis, 3D FDTD method with perfect matching layer (PML) absorbing boundary condition is used to investigate the loss property of the polariser. Gaussian pulse as the light source injects into the waveguide structure. The grid sizes in the  $x$ ,  $y$  and  $z$  directions are chosen to be  $\Delta x = \Delta y = \Delta z = 1$  nm which are sufficient for numerical convergence. The power monitors are set at Port<sub>in</sub> and Port<sub>out</sub> to detect the input power  $P_{\text{in}}$  and the transmitted power  $P_{\text{out}}$ . So the transmission can be calculated as  $T = P_{\text{out}}/P_{\text{in}}$ . Furthermore, we use IL and PER to evaluate the property of the polariser, which can be calculated as follows:

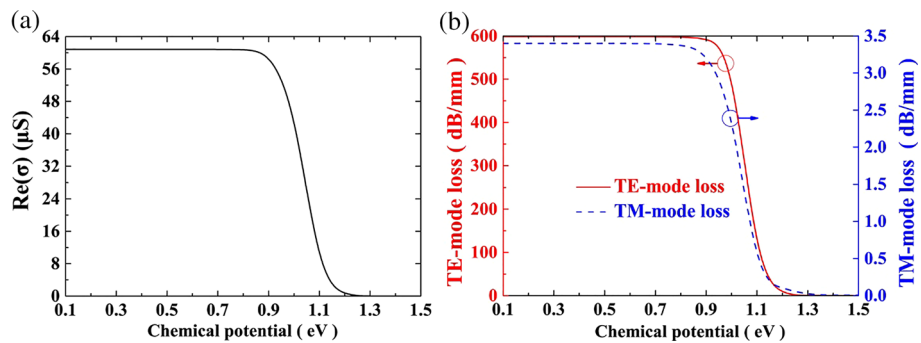
$$\text{IL} = -10 \log_{10}(T) \quad (3)$$

$$\text{PER} = 10 \log_{10}(T_{\text{TM}}/T_{\text{TE}}). \quad (4)$$

First, we investigate the relationship between the chemical potential and the loss of the two modes. Next, we investigate the relative fabrication error of the proposed polariser, where the impacts of the structure parameters are discussed.



**Figure 2.** Intensity profile in the polariser for the incident (a) TE-mode light and (b) TM-mode light. The operational wavelength of the visible light is from 300 to 600 nm. The parameters of the structure are:  $h = 10$  nm,  $h_1 = 0.5$  nm,  $h_2 = 65$  nm, and  $w = 150$  nm.



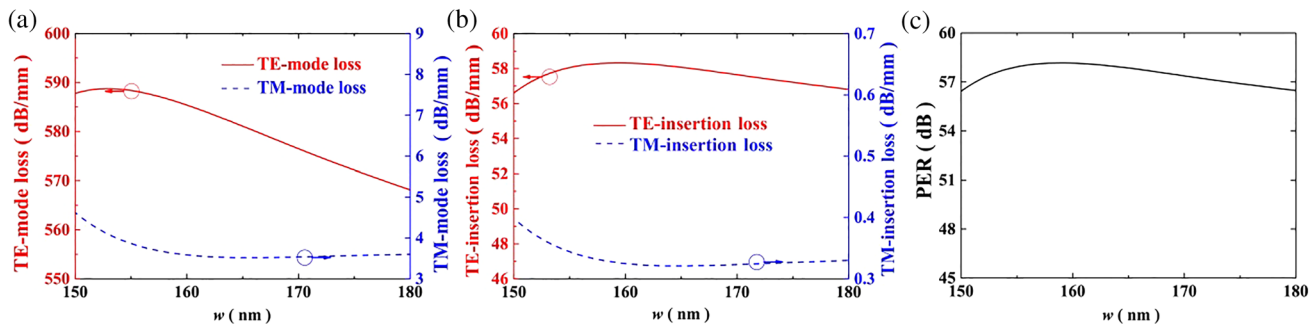
**Figure 3.** (a) The real part of surface conductivity and (b) TE-mode loss and TM-mode loss vs. the chemical potential of graphene in the polariser. The other parameters are:  $\lambda = 600$  nm,  $h = \lambda/60$ ,  $h_1 = \lambda/1200$ ,  $h_2 = 13\lambda/120$ , and  $w = \lambda/4$ .

Figure 2 shows the typical field intensity profiles for the incident TE- and TM-mode lights at the visible wavelength. The optimal structural parameters are:  $h = 10$  nm,  $h_1 = 0.5$  nm,  $h_2 = 65$  nm, and  $w = 150$  nm. It is clear that the TE-mode light is confined in the Si layer, while the TM-mode light is guided by the SiC layers.

Figure 3 shows the real part of surface conductivity  $Re(\sigma)$  and TE- and TM-mode losses as a function of the chemical potential of graphene. Here the incident wavelength is 600 nm. When the chemical potential is low ( $\mu_c < hv_0/2 \approx 1.04$  eV), interband transitions occur. When the chemical potential is high ( $\mu_c > hv_0/2 \approx 1.04$  eV), interband transitions do not occur. It is also called Pauli blocking [30]. So we can observe a quick drop of surface conductivity from 1.0 to 1.1 eV. It can also be observed that both the mode losses have a quick drop in the range from 1.0 to 1.1 eV, as shown in figure 3b. The TE- and TM-mode losses decrease while the chemical

potential increases. When the chemical potential of graphene is 0.1 eV, the TE-mode loss reaches its maximum value of 598.2 dB/mm, while the TM-mode loss is only 3.3 dB/mm, indicating that the proposed structure can be a high performance polariser. For the two polarised lights, only the field component which is parallel to the plane of the graphene can interact with graphene effectively. Therefore, if the fraction of the mode-field component parallel to graphene is higher, the absorption formed can be higher [31]. So we can obtain a high TE-mode loss and a low TM-mode loss. In the following simulations, we set the chemical potential of graphene to be 0.1 eV.

To verify the robustness of the proposed polariser, we analyse the fabrication tolerance of the waveguide width, the height of the Si and SiC layers. Figure 4 shows the calculated mode loss as a function of the waveguide width  $w$  for the polariser. As shown in figure 4a, for TE-mode light, the loss varies from 587.7 to 569.4 dB/mm



**Figure 4.** (a) The TE- and TM-mode losses, (b) the IL of the TE and TM modes, and (c) PER vs. the width of the polariser. The other parameters are:  $\lambda = 600$  nm,  $h = \lambda/60$ ,  $h_1 = \lambda/1200$ ,  $h_2 = 13\lambda/120$ , and  $\mu_c = 0.1$  eV.

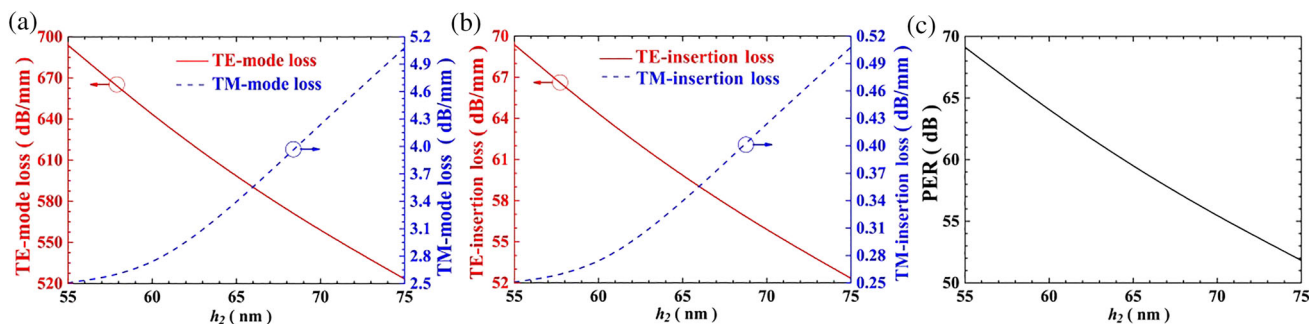


**Figure 5.** (a) The TE- and TM-mode losses, (b) the IL of the TE and TM modes, and (c) PER vs. the height of the Si layer. The other parameters are:  $\lambda = 600$  nm,  $h = \lambda/60$ ,  $h_1 = \lambda/1200$ ,  $h_2 = 13\lambda/120$ , and  $\mu_c = 0.1$  eV.

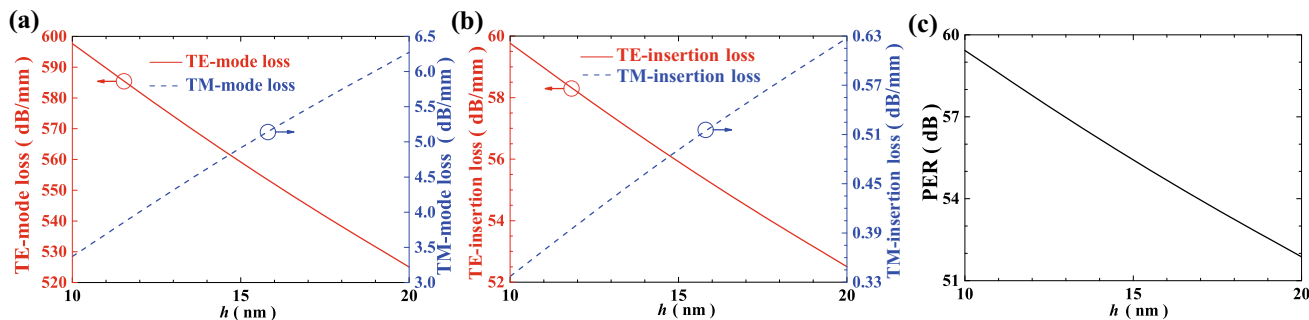
and the TM-mode loss varies from 4.8 to 3.4 dB/mm when the waveguide width changes from  $\lambda/4$  to  $3\lambda/10$ . The TM-mode loss increases while the width increases, but the TE-mode loss reaches a peak value when the width is 154 nm. Figure 4b shows that the IL of the TE mode varies from 56.8 to 58.4 dB, and the IL of the TM mode varies from 0.40 to 0.33 dB. As shown in figure 4c, by employing a 100  $\mu\text{m}$  long waveguide polariser, the PER varies from 56.5 to 58.8 dB and the percentage variation is less than 4%, which shows the great fabrication error tolerance. Generally, this TM mode-pass polariser exhibits a low IL of  $\sim 0.3$  dB for TM-mode light and a very high PER of  $\sim 57$  dB, which shows its great performance as a polariser.

Figure 5 shows the mode loss, IL and PER of the TE and TM modes as a function of the height of Si layer. As shown in figure 5a, when the height of the Si layer increases from  $11\lambda/120$  to  $\lambda/8$ , the TE-mode loss monotonically decreases from 693.8 to 523.4 dB/mm, while the TM-mode loss monotonically increases from 2.5 to 5.1 dB/mm. Moreover, as shown in figure 5b, we can observe that the IL of the TE mode varies from 69.4 to 52.3 dB, and the IL of TM mode's variation range is from 0.25 to 0.51 dB. According to figure 5c, the PER decreases from 69.1 to 51.8 dB, which still remains above 50 dB. So the polariser can exhibit good

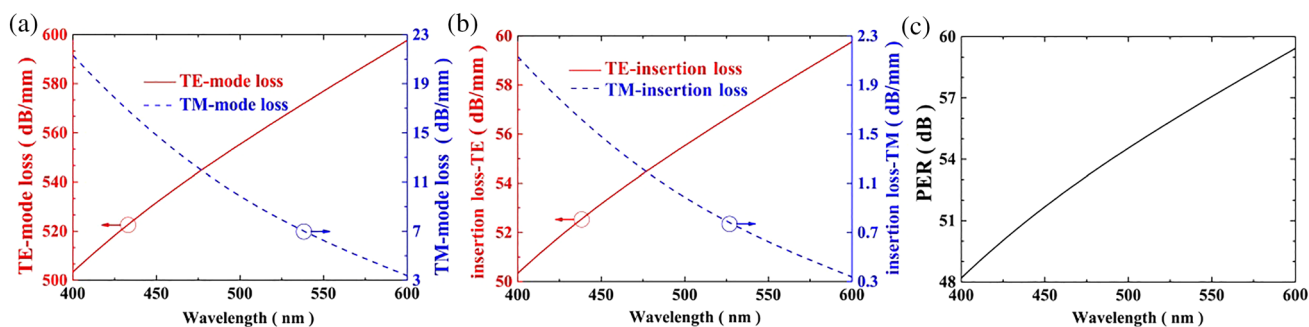
performance when the height of the Si layer changes from  $11\lambda/120$  to  $\lambda/8$ .

Figure 6 shows the calculated loss of TE and TM modes as a function of the height of the SiC layer. When the height of the SiC layer increases from  $\lambda/60$  to  $\lambda/30$ , the TE-mode loss monotonically decreases from 597.7 to 525.0 dB/mm, while the TM-mode loss monotonically increases from 3.4 to 6.3 dB/mm, as shown in figure 6a. Moreover, as shown in figure 6b, for TE mode, the IL varies from 59.8 to 52.5 dB. For TM mode, the IL varies from 0.34 to 0.63 dB. Figure 6c shows that the PER decreases from 59.4 to 51.9 dB. The percent change of PER is less than 13.7% when the height of the Si layer changes from  $\lambda/60$  to  $\lambda/30$ . From the previous discussions on the effects of structure parameter errors, we find that the performance of the polariser will not be affected when the relative fabrication error is not big, which can ensure high robustness for fabrication.

At last, we further study the wavelength sensitivity of our proposed polariser, as shown in figure 7. When the wavelength changes from 400 to 600 nm in the visible range, the TE-mode loss increases from 508.3 to 597.7.9 dB/mm, while the TM-mode loss decreases from 20.2 to 3.4 dB/mm. The IL of the TE mode varies from 50.8 to 59.8 dB and the IL of TM mode varies from 2.0 to 0.3



**Figure 6.** (a) The TE- and TM-mode losses, (b) the IL of the TE and TM modes, and (c) PER vs. the height of the SiC layer. The other parameters are:  $\lambda = 600$  nm,  $w = \lambda/4$ ,  $h_1 = \lambda/1200$ ,  $h_2 = 13\lambda/120$ , and  $\mu_c = 0.1$  eV.



**Figure 7.** (a) The TE- and TM-mode losses, (b) the IL of the TE and TM modes, and (c) PER vs. the wavelength of the incident light. The other parameters are:  $w = 150$  nm,  $h = 10$  nm,  $h_1 = 0.5$  nm,  $h_2 = 65$  nm, and  $\mu_c = 0.1$  eV.

dB. Besides, the PER varies from 48.8 to 59.4 dB. The high PER values indicate that this structure can perform very well in the visible spectrum.

### 3. Conclusions

In summary, we have proposed a graphene-assisted polariser with high PER and broad bandwidth. The numerical simulation results based on FDTD method show that the influences of different structure parameters on the performance of the polarisers are very small, which can ensure high robustness for fabrication. Besides, the IL of the TM mode input is less than 2 dB and the PER of a  $100 \mu\text{m}$  long waveguide is higher than 48.8 dB in the visible regime ranging from 400 to 600 nm, indicating great performance of the polariser in the visible range.

### Acknowledgements

This work was partially supported by the National Natural Science Foundation of China under Grant 61705058, Natural Science Foundation of Jiangsu Province under

Grant BK20170302, Changzhou Science and Technology Program under Grant CJ20179023 and Fundamental Research Fund for Central Universities of China under Grant 2019B21314.

### References

- [1] A Rahim, E Ryckeboer, A Subramanian, S Clemmen, B Kuyken, A Dhakal, A Raza, A Hermans and M Muneeb, *J. Light. Technol.* **35**, 639 (2017)
- [2] Q Bao and K Loh, *ACS Nano* **6**, 3677 (2012)
- [3] S Jahani and Z Jacob, *Nat. Nanotechnol.* **11**, 23 (2016)
- [4] B Ni and J Xiao, *IEEE J. Quantum Electron.* **53**, 1 (2017)
- [5] M Cappellar, *Annu. Rev. Astron. Astr.* **54**, 597 (2016)
- [6] Y Cheng, C Wu, Z Cheng and R Gong, *Prog. Electromagn. Res.* **155**, 105 (2016)
- [7] H Xu, S Tang, G Wang, T Cai, W Huang, Q He, S Sun and L Zhou, *IEEE Trans. Antennas Propag.* **64**, 3676 (2016)
- [8] D Kim, M Lee, Y Kim and K Kim, *Opt. Express* **24**, 21560 (2016)
- [9] K Liu, J Varghese, J Gerasimov, A Polyakov, M Shuai, J Su, D Chen, W Zajaczkowski, A Marcozzi and W Pisula, *Nat. Commun.* **7**, 11476 (2016)
- [10] S Kim, B Kim, J Lee, H Shin, Y Park and J Park, *Mater. Sci. Eng. R.* **99**, 1 (2016)

- [11] V Sharma, D Madaan and A Kapoor, *IEEE Photon. Technol. Lett.* **29**, 559 (2017)
- [12] Z Ge and S Wu, *Appl. Phys. Lett.* **22**, 121104 (2008)
- [13] T Sun, J Kim, J Yuk, A Zettl, F Wang and C Chang-Hasnain, *Opt. Express* **24**, 26035 (2016)
- [14] L Yang, T Hu, R Hao, C Qiu, C Xu, H Yu, X Jiang, Y Li and J Yang, *Opt. Lett.* **38**, 2512 (2013)
- [15] Z Huang, H Park, E Parrott, H Cha and E Pickwell-MacPherson, *IEEE Photon. Technol. Lett.* **25**, 81 (2013)
- [16] B Lee, A Mousavian, M Paul, Z Thompson, A Stickel, D McCuen, E Jang, Y Kim, J Kyoung and D Kim, *Appl. Phys. Lett.* **108**, 241111 (2016)
- [17] A Geim, *Science* **324**, 1530 (2009)
- [18] W Su and B Chen, *Pramana – J. Phys.* **89**: 37 (2017)
- [19] S M Demir, Y Yuksek and C Sabah, *Pramana – J. Phys.* **90**: 65 (2018)
- [20] K Novoselov, A Geim, S Morozov, D Jiang, M Katsnelson, I Grigorieva, S Dubonos and A Firsov, *Nature* **438**, 197 (2005)
- [21] K Bhatt, C Rani, M Vaid, P Kumar, S Kumar, S Shrivastawa, S Sharma, R Singh and C C Tripathi, *Pramana – J. Phys.* **90**: 75 (2018)
- [22] L Ming, Y Xiaobo, U Erick, G Baisong, Z Thomas, J Long, W Feng and Z Xiang, *Nature* **474**, 64 (2011)
- [23] J Kim and C Choi, *Opt. Express* **20**, 3556 (2012)
- [24] D Oliveira, E Rafael and J Christiano, *Sci. Rep. UK* **5**, 16949 (2015)
- [25] X Yin, Z Tian, C Lin and L Xun, *Opt. Lett.* **40**, 1733 (2015)
- [26] X Hu and W Jian, *IEEE Photon. J.* **9**, 1 (2017)
- [27] E D Palik, *Handbook of optical constants of solids* (Academic Press, San Diego, 1998).
- [28] S Bahadori-Haghighi, R Ghayour and M Sheikhi, *J. Light. Technol.* **35**, 2211 (2017)
- [29] P Chen, J Soric, Y Padooru, H Bernety, A Yakovlev and A Alu, *New J. Phys.* **15**, 123029 (2013)
- [30] F Wang, Y Zhang, C Tian, C Girit, A Zettl, M Crommie and Y Shen, *Science* **320**, 206 (2008)
- [31] M Kwon, *IEEE Photon. J.* **6**, 1 (2014)